

Performance Analysis and Implementation of Hybrid Conjugate Gradient Method in Electromagnetic Tomography

Michelle Ubong Sari¹, Norhaslinda Zullpakal^{1*}, Nurfatihah Anizan¹, Dzul
Dzaihan Dzul Gzailani¹, Nur Syarafina Mohamed²,

¹College of Computing, Informatics and Mathematics, Universiti Teknologi MARA Terengganu Branch, Kuala Terengganu
Campus, Terengganu Malaysia

²Department of Mathematical Sciences, Faculty of Science, Universiti Teknologi Malaysia, Johor Malaysia

ARTICLE INFO

Article history:

Received 12 March 2025

Revised 26 March 2025

Accepted 9 April 2025

Online first

Published 30 April 2025

Keywords:

Electromagnetic Tomography

Conjugate Gradient Method

Root Means Square Error

Optimization

Inverse Problem

Numerical Analysis

DOI:

10.24191/mij.v6i1.5005

ABSTRACT

Electromagnetic tomography (EMT) is a type of electrical tomography based on electromagnetic induction. Reconstructing images with EMT involves solving inverse problems, which are often poorly defined due to limited prior information about imaging features. Optimization methods such as conjugate gradient (CG), Quasi-Newton, and Steepest Descent can help minimize these problems. The conjugate gradient (CG) algorithm is an iterative method that efficiently handles equations with multiple inputs, saving time but requiring more memory. In this research, four hybrid CG methods which is MN-LAMR, MN-FR, MN-LS and MN-PRP are used to reduce the number of iterations (NOI) and CPU time, achieving excellent numerical performance. Based on numerical performances, MN-LAMR is the best method. Then, MN-LAMR is implemented into the EMT system to produce a new system called EMT-CG. The efficiency of the EMT and EMT-CG systems is evaluated based on error analysis using root mean square error (RMSE). The implementation of MN-LAMR into EMT improves its system efficiency according to the smaller number RMSE in comparison between EMT and EMT-CG. The findings highlight the hybrid CG method's capability within the EMT system which will be useful in enhancing the medical field technology.

1. INTRODUCTION

Optimization means finding the best solution among different feasible alternatives, where feasible solutions mean those that satisfy all the constraints (Kheiri, 2018). Optimization can be defined as one of the branches

^{1*} Corresponding author. E-mail address: lindazullpakal@uitm.edu.my

of knowledge dealing with finding the optimal solutions to a specific issue within a set of alternatives (Khaleel & Mitras, 2020). Unconstrained optimization consists of minimizing a function which depends on several real variables without any restrictions on the values of these variables (Andrei, 2020).

Electromagnetic tomography (EMT) is a kind of electrical tomography technology based on electromagnetic induction principle (Liu et al., 2019). The word “tomography” comes from the Greek words “tomos” which means “a slice”, “a section,” “graph,” and “image” (Wei & Soleimani, 2013). The portability of EMT systems allows for their potential exploitation in onsite medical emergencies, such as stroke or sport and road accidents. However, such a possibility is currently hindered by the high computational time that required to retrieve accurate tomographic images, as the governing equations of EMT are generally nonlinear (Xiang et al., 2020).

The conjugate gradient (CG) algorithm is an iterative method for efficiently treating equations involving multiple external forces that offer significant time savings but require more memory (Smith et al., 1989). It was stated by Nocedal and Wright (2006) that CG is among the most useful techniques for solving large linear systems of equations and can be adapted to solve nonlinear optimization problems. For instance, real-life problems that require the application of CG include portfolio optimization in finance, solving heat conditions in materials, image deblurring, and path planning in robotics. Most of the unconstrained optimization problems are solved using the CG method to avoid the high computational cost of Newton’s method and to accelerate the convergence rate of steepest descent. The CG method can be classified in 6 groups which is classical, hybrid, modified, scaled, parametrized and accelerated (Andrei, 2008). There are several types of CG coefficients such as Linda-Aini-Mustafa-Rivaie (LAMR), Hestenes - Stiefel (HS), Fletcher – Reeves (FR), Polak – Ribière – Polyak (PRP), Liu – Storey (LS) and Dai – Yuan (DY). The best CG can be selected depending on the result, where sufficient descent is achieved with lower central processing unit (CPU) time and smaller number of iteration (NOI) times.

Some common line search methods are used with CG, depending on the specific implementation and requirements of the optimization problem. The Wolfe line search algorithm is a method for finding descent directions in a scalar minimization problem when the line search satisfies the standard Wolfe conditions (Gonçalves & Prudente, 2020). The CG method is applied for solving the inverse problems of EMT to reconstruct and display the image from the measured data. In the medical field, this imaging technique utilizes electrical measurements to reconstruct the images of the internal conductivity distribution within a body. It is also considered much safer compared to certain X-ray-based imaging techniques, as ionizing radiation is not involved. For instance, the EMT can produce images of brain tumors which can help the medical field to detect cancer without having to risk the patient’s health getting exposure from the radiation.

2. LITERATURE REVIEW

Optimization plays a crucial part in solving real-life problems as it contributes to efficiency, decision-making, and resource allocation in numerous fields. The focus of this research is to check the effectiveness of different types of MN hybrid CG with LAMR, FR, LS, and PRP to find the fastest CPU time and fewer NOI before solving the inverse problem. In the inverse problem of tomography field, the solution of image reconstruction is often ill-posed and the prior information about imaging features is limited (Xiao et al., 2018). The research proceeds by conducting image reconstruction to prove the effectiveness of the new hybrid CG methods. According to Marr (1980), image reconstruction which is also known as computerized tomography is a mathematical process that generates tomographic images from X-ray projection data acquired at many different angles around the patient. There are two crucial parts for image reconstruction to success which includes the forward and inverse problem. However, this research intends to determine the success in implementing hybrid CG into the EMT system by focusing more on solving the inverse problem.

2.1 Forward Problem in EMT

According to Liu et. all (2019), the Maxwell's equation group of harmonic forms given as follows:

$$\{\nabla \times \vec{H} = \vec{J} + j\omega\vec{D} \nabla \times \vec{E} = -j\omega\vec{B} \nabla \cdot \vec{B} = 0 \nabla \cdot \vec{D} = 0 \quad (1)$$

Based on Sánchez et al. (2012), \vec{H} is the magnetic field intensity, \vec{E} is the electric field intensity, \vec{J} is the current density, \vec{D} is the electric displacement field, \vec{B} is the magnetic flux density, j is the imaginary unit and ω is the angular frequency of the harmonic excitation.

The next step is to define the magnetic vector potential which satisfies as below:

$$\nabla \times \vec{A} = \vec{B} \quad (2)$$

The purpose is to simplify the Maxwell's equations where it satisfies the condition $\nabla \cdot \vec{B} = 0$ which defined as the curl of magnetic vector potential \vec{A} . It is crucial and to be applied in the coding for accurate reconstruction of the material properties from the electromagnetic measurements.

For the distribution of the excitation coils in EMT system, the corresponding Neumann boundary conditions are determined:

$$\{\mu^{-1} \cdot \left(\frac{\partial^2 \vec{A}}{\partial x^2} + \frac{\partial^2 \vec{A}}{\partial y^2} \right) = j\omega\delta\vec{A} \frac{\partial \vec{A}}{\partial n} |_{x^2+y^2=R^2} = \mu_0 \vec{I} \quad (3)$$

where R is the radius of the circumference of the excitation coil, μ_0 is the permeability of air and \vec{I} is the current density of the excitation coil. For the first equation, the magnetic vector potential \vec{A} indicates its behavior within the domain considering the harmonic excitation. The second equation is the Neumann boundary condition that specifies the behaviour of \vec{A} on the boundary of the domain, where n denotes the outward normal direction at the boundary which ties the boundary values of \vec{A} to the current \vec{I} .

In the forward problem, the solution of sensitivity matrix is the key, and it is also an important index to solve the inverse problem which defines as below:

$$s_{ij}(k) = \frac{A_j^{(k)} - A_j(\mu)}{A_j(\mu) - A_j(\mu_0)} \cdot \frac{1}{\mu - \mu_0} \cdot \omega(k) \quad (4)$$

2.2 Inverse Problem in EMT

An inverse problem arises when the spatial sensitivity coefficient matrix of the object field formed is detected by the EMT system to obtain the value in all directions of the object.

The inverse problem of the EMT system can be defined as the following equation:

$$Sx = b \quad (5)$$

where $S \in R^{m \times n}$, $x \in R^n$, $b \in R^m$ and $m < n$.

The calculation of the corresponding objective function is performed multiple times so that it gradually approaches the optimal solution. The inverse problem is then optimized into unconstrained continuous differential equations, as shown in the result below:

$$f(x) = (Sx - b) \quad (6)$$

The iterative formula of the CG algorithm for the search direction, d_k is defined below, if the equation $f(x)$ is continuously differentiable:

$$x_{k+1} = x_k + a_k d_k \quad (7)$$

$$d_k = \begin{cases} -g_k, & k = 0 \\ -g_k + \beta_k d_{k-1}, & k \geq 1 \end{cases} \quad (8)$$

where $g(x) = f(x)$. According to Al-Namat and Al-Naemi (2020), the strong Wolfe line search conditions are required as follows:

$$f(x_k + a_k d_k) \leq f(x_k) + \sigma a_k d_k \quad (9)$$

$$|g(x_k + a_k d_k)| \leq \delta |g_k^T d_k| \quad (10)$$

where $0 < \sigma < \delta < 1$ to find an approximation of a_k . Different choices for the parameter β_k correspond to different CG methods. In this research, the chosen formula of β_k is listed in Table 1.

Table 1. List of Coefficients and its Author

No	Authors	Coefficients
1	Polar, Ribiere and Polyak (1969)	$\beta_k^{PRP} = \frac{g_k^T (g_k - g_{k-1})}{\ g_{k-1}\ ^2}$
2	Liu and Storey (1991)	$\beta_k^{LS} = \frac{g_k^T (g_k - g_{k-1})}{d_{k-1}^T g_{k-1}}$
3	Linda, Aini, Mustafa and Rivaie (2017)	$\beta_k^{LAMR} = \frac{g_k^T \left(\frac{\ d_{k-1}\ }{\ d_{k-1} - g_k\ } g_k - g_{k-1} \right)}{\frac{\ d_{k-1}\ }{\ d_{k-1} - g_k\ } \ d_{k-1}\ ^2}$
4	Fletcher-Reeves (1964)	$\beta_k^{FR} = \frac{\ g_k\ ^2}{\ g_{k-1}\ ^2}$

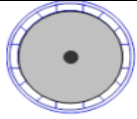
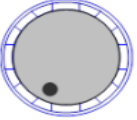
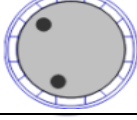
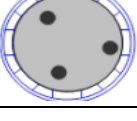
2.3 Monarchy Metaheuristic (MN)

The most important aspect of the research is the utilization of this hybrid CG algorithm to demonstrate successful real-world applications. A new CG coefficient, MN was proposed by Liu et al. (2019) which improve the convergence of the algorithm, increase the step size, reduce NOI and shorten the CPU time. The MN conjugate coefficient is defined as below:

$$\beta_k^{MN} = \frac{\|g_k\|^2 - \{0, g_k^T, g_{k-1}\}}{\{\|g_{k-1}\|^2, d_{k-1}^T y_{k-1}\}} \quad (11)$$

As the hybrid CG aims to enhance the performance of the method, a hybridization process takes place, followed by a comparison for each hybrid CG with the new MN coefficient. According to Liu et al (2019), the numerical test using different images are done as in Table 2 where M, I, T and S respectively represent the name of the CG algorithm, NOI, CPU time and the termination condition of the algorithm. When S=1, it means that the system can be solved using hybrid CG while S=0 indicates that the implementation of hybrid CG is failed.

Table 2. Numerical Test with Four Different Images

Original Image	M	I	T/s	S
	PRP	78	64.2134	1
	HCG	45	51.4252	1
	MN	34	40.1254	1
	PRP	64	65.7658	1
	HCG	47	56.1543	1
	MN	36	39.7853	1
	PRP	88	71.0346	1
	HCG	78	58.5655	1
	MN	67	49.9987	1
	PRP	80	65.7789	1
	HCG	79	70.3475	1
	MN	45	37.9801	1

2.4 EMT Applications

It was stated by Khan and Ling (2019) that EMT, also known as electrical impedance tomography (EIT) is a new imaging method involving the injection of a small amount of current to determine the electrical properties of tissues and to measure the resulting voltages. It is safe to say that EMT is better than magnetic resonance imaging (MRI) and computed tomography (CT) because EMT in nature is non-invasive and constructs radiation free images.

EIT has an advantage over the other imaging techniques such as its portability, low-cost and faster imaging capabilities (Khan & Ling, 2019). Ever since the potential use of EMT or EIT as an imaging model is recognized in the medical field, an improvement in EMT through hybridization due to its low spatial resolution, which can impact the ability to precisely locate structures or abnormalities within the body, and the ill-posed nature of the image reconstruction involving a complex mathematical inverse problem can be achieved. Therefore, the hybridization of EMT with the best hybrid CG can contribute to improving the performance by reducing the CPU time, producing less NOI and increasing the speed of convergence.

2.5 Discussion on Hybrid Conjugate Gradient Method for EMT Applications

Based on Liu et al. (2019), MN hybrid CG method improved image reconstruction by reducing the NOI and CPU time compared to traditional CG methods. The previous study successfully demonstrates that hybrid CG approaches can optimize EMT application by enhancing computational efficiency, reducing convergence time and providing systemic comparison of PRP, HCG and MN methods which highlighting the effectiveness of hybrid approaches in EMT. However, it has limited evaluation scope by using small number of test cases, lack of alternative hybridization strategies as it mainly focuses on MN-based hybrid CG and lack of structured error analysis.

This study builds upon Liu et al. (2019) work by broadening the scope of hybrid CG methods and providing a quantitative error analysis performance evaluation using RMSE. To address the limitations on Liu et. al (2019) study, multiple hybrid CG methods is tested to identify the best approach to the EMT and exploring broader test cases and diverse image structures to enhance generalizability. This study also aims to refine existing methods and provide a more robust solution for EMT applications further ensures that the best-performing algorithm leading to improved imaging accuracy and computational efficiency.

This study uses the RMSE as performance metrics to evaluate the accuracy of EMT image application by measuring the difference between the reconstructed image and the original image. A lower RMSE indicates higher reconstruction accuracy by comparing different optimization methods between EMT and EMT-CG and determining the best approach for EMT applications.

Successful hybridization of EMT-CG has significant implications for EMT application especially in medical imaging which demanded accuracy and fast reconstruction of conductivity distribution for applications such as brain stroke detection, breast cancer screening and lung function assessment. EMT-CG improved image reconstruction speed which allows quicker stroke diagnosis using EMT, a non-invasive monitoring of tissue conductivity changes as it benefits from fast convergence methods and enhance accuracy of respiratory monitoring.

3. METHODOLOGY

3.1 New Hybrid Conjugate Gradient Method and Algorithm

MN is chosen to combine with four different β_k coefficients, which are PRP, LS, LAMR and FR. The new methods for hybrid CG are stated as below:

$$\beta_k^{MN-LAMR} = \{\beta_k^{MN} \quad \text{if} \quad 0 \leq \beta_k^{LAMR} \leq \beta_k^{MN} \beta_k^{LAMR} \quad \text{otherwise} \quad (12)$$

$$\beta_k^{MN-PRP} = \{\beta_k^{MN} \quad \text{if} \quad 0 \leq \beta_k^{PRP} \leq \beta_k^{MN} \beta_k^{PRP} \quad \text{otherwise} \quad (13)$$

$$\beta_k^{MN-LS} = \{\beta_k^{MN} \quad \text{if} \quad 0 \leq \beta_k^{LS} \leq \beta_k^{MN} \beta_k^{LS} \quad \text{otherwise} \quad (14)$$

$$\beta_k^{MN-FR} = \{\beta_k^{MN} \quad \text{if} \quad 0 \leq \beta_k^{FR} \leq \beta_k^{MN} \beta_k^{FR} \quad \text{otherwise} \quad (15)$$

The names of each hybrid CG method will be represented by MN-PRP, MN-LS, MN-LAMR and MN-FR respectively upon successful hybridization of MN with each of the four different β_k coefficients by conducting numerical analysis. According to Trefethen (1992), the definition of numerical analysis is about study of algorithms for the problems of continuous mathematics that involves real or complex variables which may be impossible to solve analytically. Hence, numerical analysis helps to determine the accuracy, precision, stability, convergence and visualization for the research.

The algorithm for numerical test is below,

Step 1: Initialization. Given x_0 , set $k = 0$.

Step 2: Selection of initial points $x_1 \in R^n$, set $k = 1$ and calculate $g_1 = g(x_1)$.

Step 3: If $\|g_k\| < \varepsilon$, then iteration stop.

Step 4: Set $x_{k+1} = x_k + a_k d_k$ and $g_{k+1} = g(x_{k+1})$.

Step 5: Computing hybrid CG coefficient.

Computing β_k based on the formula.

Step 6: Computing search directions, $d_k = -g_k + \beta_k d_{k-1}$

If $g_k = 0$, then stop.

Step 7: Computing step size. Solve $a_k = f(x_k + a d_k)$.

Step 8: Updating new point, $x_{k+1} = x_k + a_k d_k$.

Step 9: Convergent test and stopping criteria.

If $f(x_{k+1}) < f(x_k)$ and $\|g_k\| < \varepsilon$ then stop. Otherwise go to step 1 with $k = k + 1$.

4. RESULTS AND DISCUSSION

Four CG coefficients are chosen for numerical testing by solving 15 standard test functions which are listed in Table 3.

Table 3. List of Standard Test Functions

No.	Test Function	Variables	Initial Points
1	Extended White & Holst	2, 4, 10, 100, 500, 1000	(-4,...,-4), (-2,...,-2), (2,...,2), (8,...,8)
2	Extended Tridiagonal 1	2, 4, 10, 100	(-2,...,-2), (4,...,4), (14,...,14), (21,...,21)
3	Diagonal 4	2, 4, 10, 100, 500, 1000	(-2,...,-2), (4,...,4), (14,...,14), (21,...,21)
4	Extended Himmelblau	2, 4, 10, 100, 500, 1000	(-4,...,-4), (2,...,2), (4,...,4), (21,...,21)
5	Extended Powell	2, 4, 10, 100, 500, 1000	(-2,...,-2), (4,...,4), (14,...,14), (21,...,21)
6	NONSCOMP	2, 4, 10, 100, 500, 1000	(-4,...,-4), (4,...,4), (7,...,7), (22,...,22)
7	Extended DENSCHNB	2, 4, 10, 100, 500, 1000	(-2,...,-2), (4,...,4), (14,...,14), (21,...,21)
8	Extended Quadratic Penalty QP1	2, 4, 10	(-4,...,-4), (2,...,2), (4,...,4), (14,...,14)
9	Shallow	2, 4, 10, 100, 500, 1000	(-2,...,-2), (2,...,2), (4,...,4), (14,...,14)
10	Quadratic QF2	2, 4, 10, 100, 500, 1000	(-2,...,-2), (2,...,2), (14,...,14), (22,...,22)
11	Generalized Tridiagonal 1	2, 4, 10, 100	(-4,...,-4), (-2,...,-2), (14,...,14), (21,...,21)
12	POWER	2, 4, 10, 100	(-2,...,-2), (2,...,2), (4,...,4), (14,...,14)
13	Quadratic QF1	2, 4, 10, 100, 500, 1000	(2,...,2), (4,...,4), (14,...,14), (21,...,21)
14	Sphere	2, 4, 10, 100, 500, 1000	(-2,...,-2), (2,...,2), (4,...,4), (14,...,14)
15	Sum Squares	2, 4, 10, 100, 500, 1000	(2,...,2), (4,...,4), (14,...,14), (21,...,21)

All these methods are tested using strong Wolfe line search using MATLAB2022b programming are recorded. The results of the NOI and CPU for each hybrid CG are interpreted into performance profile proposed by Dolan and Moré (2002). In performance profile, the curve line at the top left of the graph indicates the fastest method with the smallest NOI or CPU time while the curves at the right side of the graph indicates the amount of test functions successfully solved by the methods which also indicates the robustness of the method.

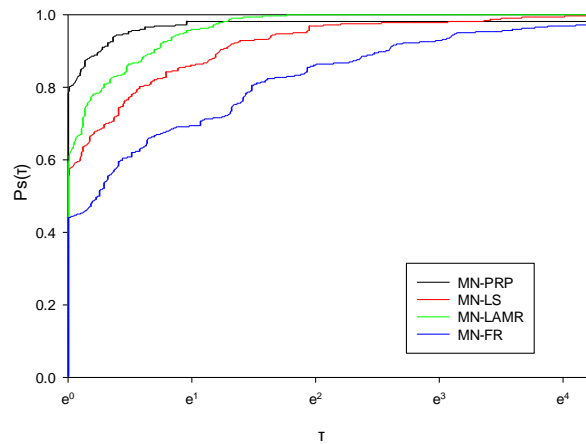


Fig. 1. Numerical Results of NOI

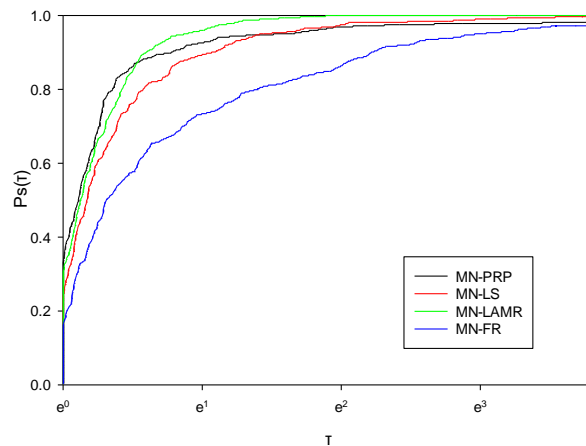


Fig. 2. Numerical Results of CPU Time

Fig. 1 and Fig. 2 show the performance profile for all the hybrid CG methods in terms of NOI and CPU time respectively. Based on Figure 3, the MN-PRP is the fastest, but MN-LAMR is more robust than MN-PRP. Through closer inspection, MN-PRP is the most efficient method since it has the highest curve as followed by MN-LAMR, MN-LS and MN-FR. At certain times, MN-LAMR takes over MN-PRP method. MN-PRP is the fastest method among the other three hybrid CG, but it is unable to solve many test functions. Based on Figure 5.1 and Figure 5.2, MN-LAMR converges significantly faster with lowest NOI means faster computation and lower CPU time which improves real-time imaging. With the overall 325 test problems, the summarized results of all the hybrid CG methods are recorded in Table 4.

Table 4. Percentage of Test Function Successfully solved by Tested Hybrid CG Methods

No	Methods	Percentage (%)
1	MN-LAMR	100.0
2	MN-LS	99.7
3	MN-PRP	98.1
4	MN-FR	97.2

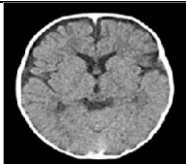

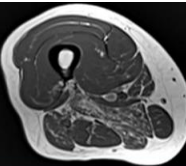
As shown in Table 4, MN-LAMR solves 100% test problems and this result is followed by MN-LS, MN-PRP and MN-FR that are able to solve 99.7%, 98.1% and 97.2% test problems respectively. Thus, it is concluded that MN-LAMR is the best coefficient out of four hybrid CG.

Then, the best hybrid CG method which is MN-LAMR is applied into the EMT system. Using three different images for reconstruction purposes, the MN-LAMR method is expected to solve the inverse problem in EMT system. The results are compared with the original solution for EMT system using MN algorithm based on the RMSE. The formula of the RMSE is as follows:

$$RMSE = \sqrt{\frac{1}{n} \sum_{i=1}^n (e_i)^2} \quad (16)$$

The performance of EMT and EMT-CG based on the result of (16) obtained from the output of image reconstruction programming are compared in Table 5.

Table 5. RMSE for Different Images

Images	RMSE	
	EMT	EMT-CG
 Brain	0.8061	0.8132
 Lung	15.0136	13.5611
 Arm	0.8747	0.8695

The difference of RMSE between the EMT and EMT-CG is so subtle because the values of RMSE are so close for both systems. However, EMT-CG best two results out of three selected pictures which indicates that EMT-CG system is better than EMT system. This suggests that the implementation of hybrid CG coefficient into the EMT system is successful. The approach to implement hybrid CG as an alternative to reconstruct the image is possible through this research.

The improvements of EMT-CG in convergence speed, computation time and accuracy is useful in real-life applications. For instance, faster scans for emergency care as it provides quicker processing for real-time monitoring, better accuracy in detecting health problems as lower RMSE values show that EMT-CG produces clearer and more detailed images which help in detecting tumours or cancer earlier.

5. CONCLUSION

The results highlight the effectiveness of the MN-LAMR method in electromagnetic tomography proven that MN-LAMR was the most efficient hybrid CG method by outperforming other tested methods in terms of NOI and CPU time. The implementation of EMT-CG significantly improves image reconstruction accuracy as shown by smaller result than EMT using RMSE analysis making it more suitable for practical applications. Overall, the implementation of CG method ion electromagnetic tomography is successful providing solution to improve inverse problem-solving techniques in image reconstruction of EMT.

6. ACKNOWLEDGEMENTS/FUNDING

The authors would like to acknowledge the support of Universiti Teknologi Mara (UiTM) Terengganu Branch, Kuala Terengganu Campus for providing the facilities and financial support on this research.

7. CONFLICT OF INTEREST STATEMENT

The authors agree that this research was conducted in the absence of any self-benefits, commercial or financial conflicts and declare the absence of conflicting interests with the funders.

8. AUTHORS' CONTRIBUTIONS

Michelle Ubong Sari carried out the research, wrote and revised the article. Nurfatihah Anizan and Dzul Dzaihan conceptualised the central research idea and provided the numerical results. Nur Syarafina Mohamed designed the research, supervised research progress; Norhaslinda Zullpakkal anchored the review, revisions and approved the article submission.

REFERENCES

- Ahmia, I., & Aider, M. (2019). A novel metaheuristic optimization algorithm: the monarchy metaheuristic. *Turkish Journal of Electrical Engineering and Computer Sciences*, 27(1), 362-376. <http://dx.doi.org/10.3906/elk-1804-56>
- Al-Namat, F. N., & Al-Naemi, G. M. (2020). Global convergence property with inexact line search for a new hybrid conjugate gradient method. *Open Access Library Journal*, 7(2), 1-14. <http://dx.doi.org/10.4236/oalib.1106048>
- Andrei, N. (2008). *conjugate gradient algorithms for unconstrained optimization. A survey on their definition*. <https://camo.ici.ro/neculai/OPT-Andrei.pdf>
- Andrei, N. (2020). *Nonlinear conjugate gradient methods for unconstrained optimization*. Springer. <https://link.springer.com/book/10.1007/978-3-030-42950-8>
- Dolan, E. D., & Moré, J. J. (2002). Benchmarking optimization software with performance profiles. *Mathematical programming*, 91, 201-213. <https://doi.org/10.1007/s101070100263>
- Gonçalves, M. L., & Prudente, L. (2020). On the extension of the Hager–Zhang conjugate gradient method for vector optimization. *Computational Optimization and Applications*, 76(3), 889-916. <https://doi.org/10.1007/s10589-019-00146-1>
- Khaleel, L. R., & Mitras, B. A. (2020). Hybrid whale optimization algorithm with modified conjugate gradient method to solve global optimization problems. *Open Access Library Journal*, 7(6), 1-18. <http://dx.doi.org/10.4236/oalib.1106459>
- Khan, T. A., & Ling, S. H. (2019). Review on electrical impedance tomography: Artificial intelligence methods and its applications. *Algorithms*, 12(5), 88. <https://doi.org/10.3390/a12050088>
- Kheiri, F. (2018). A review on optimization methods applied in energy-efficient building geometry and envelope design. *Renewable and Sustainable Energy Reviews*, 92, 897-920. <https://doi.org/10.1016/j.rser.2018.04.080>
- Liu, L., Lei, W., & Zhanjun, W. (2019). Application of Hybrid Conjugate Gradient Algorithms in Inverse Problems of Electromagnetic Tomography. *Journal of Physics: Conference Series*. <http://dx.doi.org/10.1088/1742-6596/1187/2/022028>
- Marr, R. (1980). Overview of image reconstruction. Proceedings of the International Symposium on Ill-Posed Problems. <https://www.osti.gov/biblio/5404987>
- Sánchez, C. C., Glover, P., Power, H., & Bowtell, R. (2012). Calculation of the electric field resulting from human body rotation in a magnetic field. *Physics in Medicine & Biology*, 57(15), 4739. <http://dx.doi.org/10.1088/0031-9155/57/15/4739>
- Smith, C. F., Peterson, A. F., & Mittra, R. (1989). A conjugate gradient algorithm for the treatment of multiple incident electromagnetic fields. *IEEE Transactions on Antennas and Propagation*, 37(11), 1490-1493. <https://doi.org/10.1109/8.43571>

- Trefethen, L. N. (1992). *The definition of numerical analysis*. <https://cims.nyu.edu/~oneil/courses/sp18-math252/trefethen-def-na.pdf>
- Wei, H.-Y., & Soleimani, M. (2013). Electromagnetic tomography for medical and industrial applications: Challenges and opportunities [point of view]. *Proceedings of the IEEE*, 101(3), 559-565. <https://doi.org/10.1109/JPROC.2012.2237072>
- Xiang, J., Dong, Y., & Yang, Y. (2020). Multi-frequency electromagnetic tomography for acute stroke detection using frequency-constrained sparse Bayesian learning. *IEEE Transactions on medical imaging*, 39(12), 4102-4112. <https://doi.org/10.1109/tmi.2020.3013100>
- Xiao, J., Liu, Z., Zhao, P., Li, Y., & Huo, J. (2018). Deep learning image reconstruction simulation for electromagnetic tomography. *IEEE Sensors Journal*, 18(8), 3290-3298. <https://doi.org/10.1109/JSEN.2018.2809485>



© 2023 by the authors. Submitted for possible open access publication under the terms and conditions of the Creative Commons Attribution (CC BY) license (<http://creativecommons.org/licenses/by/4.0/>).